Specific Interaction between Chitosan and Matrix Metalloprotease 2 Decreases the Invasive Activity of Human Melanoma Cells

Christian Gorzelanny,[†,‡] Birgit Pöppelmann,[†] Elwira Strozyk,[†] Bruno M. Moerschbacher,[‡] and Stefan W. Schneider[†,*]

Department of Dermatology, University of Münster, von-Esmarch Strasse 58, 48149 Münster, Germany, and Department of Plant Biochemistry and Biotechnology, University of Münster, Hindenburgplatz 55, 48143 Münster, Germany

Received March 21, 2007; Revised Manuscript Received July 12, 2007

The crucial event in metastasis is tumor invasion which in the case of melanoma cells is dependent on matrix metalloprotease 2 (MMP2). Chitosan (MW ca. 5×10^5 g mol^{-1}, degree of acetylation ca. 30%) attenuated the invasive activity of melanoma cells in a cell-based invasion assay and reduced MMP2 activity in the supernatant of melanoma cells. While the expression level of MMP2 was not affected, the amount of MMP2 in the cell supernatant was reduced, indicating a posttranscriptional effect of chitosan on MMP2. Atomic force microscopy revealed a direct molecular interaction between MMP2 and chitosan forming a complex with a diameter of 349.0 ± 69.06 nm and a height of 26.5 ± 11.50 nm. Affinity chromatography revealed a high binding-specificity of MMP2 to chitosan, and a colorimetric MMP2 activity assay suggests a noncompetitive inhibition of MMP2 by chitosan. The possible use of chitosan as a new type of MMP2 inhibitor is discussed.

Introduction

Chitosan, a chemical derivate of chitin, is composed of *N*-acetylglucosamine and glucosamine units linked via β-1.4-glycosidic bonds. The physicochemical properties of chitosans are mainly determined by their degree of acetylation (DA), reflecting the fraction of *N*-acetylglucosamine units within the chitosan molecules, and by their molecular weight or degree of polymerization (DP). Chitosan is a versatile biopolymer known for its biocompatibility and biodegradability; it possesses interesting biological activities, and a broad range of promising applications for chitosan in the life sciences have been proposed.[1,2] Many studies are available that suggest medical applications of chitosan or chitosan-based products such as nanocapsules for drug and gene delivery, and sponges or hydrogels for tissue engineering or wound healing purposes.[3]

Recent data show that chitosan within a three-dimensional sponge can ensure long-term cultivation of human osteoblasts leading to mineralization of the sponge.[4] Chitosan as a component of wound dressings is also known to be responsible for improved wound healing, possibly by enhancing proliferation of human fibroblasts.[5] However, bioactivities of chitosan tend to be difficult to reproduce, and detailed knowledge on structure/function relationships is not available. One area of particular interest troubled by contrasting reports is the bioactivity of chitosans toward tumor cells. While chitosan has been shown to induce apoptosis in human bladder tumor cells,[6] chitosan sponges have been suggested as a suitable matrix for the cultivation of human breast cancer cells to study the effects of anticancer drugs.[7,8] Possibly the bioactivity of chitosan differs with the type of tumor cell under investigation.

The purpose of this study was to investigate the impact of chitosan on melanoma cells with a focus on melanoma cell invasive properties. To our knowledge, no report is available investigating the effects of pure chitosan on melanoma cells. Previously, we have shown that matrix metalloproteases (MMPs) in general and MMP2 in particular play a pivotal role in melanoma tumor progression.[9−11] Interestingly, it has been reported recently that chitosan may suppress MMP2 expression in human fibroblasts.[12] Many different MMPs have been described in humans, and each of these proteases is unique in its substrate spectrum, regulation, and function.[13] MMPs are crucial players in different physiological contexts such as wound healing[14] but also in pathological processes such as metastasis.[15,16] Moreover, recent data demonstrate that inhibition of MMP2 secretion attenuates melanoma cell invasion significantly.[17] The present report provides structural and functional data implying that chitosan binds to melanoma-derived MMP2 accompanied by a decrease of MMP2 activity in the melanoma cell supernatant. The specificity of chitosan−MMP2 binding was shown by affinity chromatography. Using a cell-based invasion assay, we in addition observed on a cellular level that chitosan treatment reduces the invasive activity of melanoma cells.

Experimental Section

Cells and Cell Culture. The cell based migratory assay consisted of two cell types, namely the highly malignant, actin binding protein-transfected human amelanotic melanoma cell line, subclone A7,[18] and the nonmalignant epithelial, MDCK-C7 cells.[19] Both cell lines were cultured under standard conditions as previously described.[20] To prevent contamination, penicillin (100 U mL^{-1}) and streptomycin (100 μL mL^{-1}) were present in the cell culture medium. Geneticin G148 (355 μg mL^{-1}, Life Technologies, Morelbeke, Germany) was used to select transfected A7 melanoma cells.

Proliferation Assay. The cell proliferation assay was performed as previously reported.[21] Briefly, melanoma cells were seeded onto a 96 well plate (10×10^4 cells per well) and cultured for 1 day under the

* Corresponding author. E-mail: sschnei@mednet.uni-muenster.de.
† Department of Dermatology.
‡ Department of Plant Biochemistry and Biotechnology.

10.1021/bm0703214 CCC: $37.00
Published on Web 09/11/2007

above-described conditions. Prior to the proliferation assay, the culture medium was exchanged with a serum-free medium. Cells were incubated with MTT-containing buffer for 4 h. Subsequently, cells were permeabilized, and the formazan crystals were dissolved by incubation for 24 h in the cell permeabilization buffer containing 50% DMF. The relative amount of formazan was measured photometrically at a wavelength of 470 nm. The initial OD measured for time point $t = 0$ h in the control sample corresponds to a proliferation index value of one.

Melanoma Cell Invasion Assay. The invasive properties of melanoma cells were investigated by a cell-based assay. An epithelial MDCK−C7 cell monolayer on the reverse site of a thin filter membrane (growth area, 4.2 cm^2; pore diameter, 0.4 μm; thickness, 20 μm; Falcon, Heidelberg, Germany) served as a test barrier for malignant cells due to the development of a high transepithelial electrical resistance (TEER), which was measured continuously using a STX-2 electrode (WPI, Sarasota, FL). Permeabilization of the epithelial cell layer (MDCK-C7 cells) due to the invasive activity of the tested cells can be determined by transepithelial electrical resistance (TEER) measurements, as previously reported.[9,20] Melanoma cells (1×10^6 cells) were added to the MDCK monolayer after TEER had reached a value of about 15000 Ω cm^2. The time point of melanoma cell addition was defined as 0 h. Culturing of cells was performed as described above. TEER index reflects the relative change of electrical resistance. Values below 1 indicate a decrease of resistance, and values above 1 indicate that the resistance was increased relative to time point 0 h. A resistance breakdown due to the migratory activity of melanoma cells occurred between 20 and 25 h in relation to time point 0 h.

MMP2 Expression Analysis. Expression of MMP2 was analyzed using RT-PCR. Total RNA was extracted from cells using GIT-buffer (4 M guanidinium isothiocyanate; 1% *N*-lauroylsarcosine; 100 mM 2-mercaptoethanol; 10% NaAc, pH 4.8) followed by phenol/chloroform extraction.[22] Following DNase I digestion (RQ1 DNase, Promega, Madison, WI), 2.5 μg of RNA was reversely transcribed into cDNA using RevertAid First Strand cDNA Synthesis Kit (Fermentas Inc., Burlington, Canada) as recommended by the manufacturer. Briefly, RNA and oligo-dT primer were incubated to allow hybridization in a volume of 12 μL at 70 °C for 5 min. After the mixture was chilled on ice and spun for a short time, the following components were added: reaction buffer; dNTP mix to a final concentration of 1 mM each, RNasin (recombinant ribonuclease inhibitor) 1 U μL^{-1}; M-MuLV reverse transcriptase 10 U μL^{-1}. The reaction was carried out in a final volume of 20 μL at 42 °C for 60 min. Polymerase chain reaction was carried out using primers specific to the MMP-2 gene in a 20 μL reaction volume utilizing the Red Taq Polymerase system from Sigma (St Louis, MO).[23] Specific gene expression in different samples was compared to the constitutive expression level of β-actin mRNA. To verify that the subsequent reactions were performed in the linear range of amplification, serial dilutions of template cDNA were made for each primer pair starting with 100 ng. The following primer sets were used: β-actin: F: 5′-AGAAAATCTGGCACCACACC-3′; R: 5′-CCATCTCT-TGCTCGAAGTCC-3′; MMP-2: F: 5′-TTTGATGGCATCGCTCA-GATC-3′; R: 5′-CCGCATCAATCTTTTCCGG-3′. PCR products were separated electrophoretically on 1.8% agarose gels in 1 x TAE buffer (40 mM Tris-acetate, 1 mM EDTA). The intensity of ethidium bromide-stained bands of specific products was recorded using Phoretix Grabber software (Nonlinear Dynamics, Newcastle upon Tyne, UK). To semiquantify the relative amounts of gene transcripts, the signal intensity of specific PCR products was compared to β-actin PCR products amplified from the same cDNA template in a separate PCR reaction.

Protein Preparation and Separation. To analyze proteins of human melanoma cells that were secreted into the cell supernatants, the supernatant was harvested. Cell supernatants were generated in serum-free medium or in physiological HEPES buffer (10 mM HEPES, 130 mM NaCl, 10 mM KCl, 1 mM $CaCl_2$, 1 mM $MgCl_2$). Proteins of the cell supernatant were precipitated by adding 200 μL of a 50% aqueous TCA (trichloric acid) solution (v/v) to 1 mL of supernatant. Precipitated proteins were washed carefully with 100% acetone and finally resolved in 30 μL of SDS-PAGE (sodium dodecyl sulfate−polyacrylamide gel electrophoresis) loading buffer (0.125 M Tris/HCl, pH 6.8, 4% (w/v) SDS, 10% (v/v) glycerol, 0.04% (w/v) bromophenol blue). Prior to immunoblotting or gelatin zymography, proteins were separated by SDS-PAGE according to their molecular weight. Accurate separation of MMP2 was achieved by a polyacrylamide content of 10%. To ensure comparability of individual samples, the electrophoresis gel was always loaded with the same volume of the supernatant. Protein bands were stained by silver[24] or Coomassie Brilliant Blue.[25]

Gelatin Zymography. Gelatinolytic activity of melanoma cell-derived supernatant proteins was detected by gelatin zymography. Gelatin concentration within the SDS-PAGE gel was 0.2% (w/v). After protein separation, SDS was removed from the gel by two washing steps with aqueous 2.5% (v/v) Triton X-100. After electrophoresis, the protease activity was developed by incubating the gel for 16 h at 37 °C in a 50 mM Tris-HCl buffer (50 mM Tris-HCl, 200 mM NaCl, 10 mM $CaCl_2$; pH 7.6). After Coomassie staining of the gel, gelatinolytic activity was visible as a bright band.

Immuno Blotting. Proteins separated by SDS-PAGE were blotted onto a nitrocellulose membrane and incubated with a specific antibody directed against MMP2 (Chemicon, Hampshire, United Kingdom). Binding of the specific MMP2 antibody was detected with horseradish peroxidase-conjugated secondary antibodies (Amersham, Buckinghamshire, UK). Binding of the secondary antibody was quantified using a chemiluminescense detection system (SuperSignals West Pico, Pierce Biotechnology Inc., Rockford, IL).

Atomic Force Microscopy. Samples were prepared by dropping 2 μL of the desired solution (MMP2, chitosan, or MMP2 + chitosan) onto a freshly cleaved mica surface. Molecules were adsorbed to the mica surface for 1 min. Subsequently, the surface was washed carefully with about 5 mL of ultrapure water (Millipore, Hampshire, United Kingdom; filtered subsequently through a 0.22 μm pore filter). Air-dried samples were scanned using a JPK Nanowizard atomic force microscope (JPK instruments, Berlin, Germany) in tapping mode using cantilevers with a force constant at about 10 N m^{-1} and resonance frequency in the range of 120 kHz (NSC35, Micromash, Tallinn, Estonia). Dimensions of the scanned objects in lateral extension were generally overestimated because of the tip curvature.[26] Therefore, values of the lateral extension were measured at half-maximal height of the observed object. Molecular volumes of MMP2 molecules were calculated on the basis of the measured dimensions and according to the molecular weight as previously reported.[26,27]

Binding Analysis. Binding of melanoma cell-derived supernatant proteins to chitosan was investigated by affinity chromatography. Affinity columns were composed of macroscopic chitosan beads. The degree of acetylation of chitosan (Sigma-Aldrich, Germany) was about 15%. Prior to use, chitosan was purified. Briefly, chitosan (3% w/v) was dissolved in acetic acid (2% v/v) overnight and passed through a 0.45 μm pore filter twice. Filtered samples were precipitated by the addition of sodium hydroxide (40% w/v) and incubated for 2 h at 80 °C under stirring. Sodium hydroxide was removed by several washing steps with ultrapure water. Finally, the purified chitosan was freeze-dried. To produce macroscopic chitosan beads, the freeze-dried chitosan was dissolved in acetic acid as above. Amorphous particles were formed immediately when a viscous chitosan solution was added dropwise to a 1 M sodium hydroxide solution. The solution was stirred at low speed, and particles remained in the sodium hydroxide solution for about 1 h. Recovered particles were washed carefully several times with ultrapure water, to remove sodium hydroxide completely, and packed into a column. The affinity column contained about 30 mg of chitosan. The column was loaded with 4 mL of melanoma cell-derived supernatant generated in HEPES buffer (10 mM HEPES, 130 mM NaCl, 10 mM KCl, 1 mM $CaCl_2$, 1 mM $MgCl_2$). The loaded column was eluted with eight 1-mL fractions of the HEPES buffer. The two last elution steps were performed with a HEPES buffer containing 1% (w/v) SDS to

recover all column-bound proteins. The collected fractions were further analyzed by SDS-PAGE and gelatin zymography, as described above.

MMP2 Activity Assay. The influence of chitosan on the hydrolytic activity of recombinant MMP2 (Chemicon, Hampshire, United Kingdom) was investigated using a colorimetric assay, as follows. A synthetic thiopeptolide with the sequence Ac-Pro-Leu-Gly-[2-mercapto-4-methylpentanoyl]-Leu-Gly-OC_2H_5 (BIOMOL International, USA) served as a substrate.[28] Cleavage of the thiopeptolide by MMP2 produces a sulfhydryl residue that reacts with 5,5′-dithiobis(2-nitrobenzoic acid) (DTNB) to form 2-nitro-5-thiobenzoic acid (NTB). Generation of NTB was measured at a wavelength of 405 nm by a microtiter plate spectrophotometer. Optical density was converted into molar quantity of generated product using pure NTB solutions as a standard. Prior to the spectrophotometric measurement, MMP2 was incubated for 30 min at 37 °C in the reaction buffer (10 mM HEPES, 130 mM NaCl, 10 mM KCl, 1 mM $CaCl_2$, 1 mM $MgCl_2$, 1 mM DTNB) containing chitosan or water but no substrate. The enzymatic reaction was started in the microtiter plate by addition of the substrate. Generation of NTB was monitored over a period of 30 min at 37 °C. Maximum turnover rate of the substrate, V_{max}, and the substrate concentration at $^1/_2$ V_{max}, K_{50} were obtained by nonlinear regression analysis of the data set applying the Hill equation. The Hill coefficient n_H representing the cooperativity of the substrate binding was determined by Hill plot analysis.

Results and Discussion

Chitosan-Treated Melanoma Cells Show Impaired Invasive Properties. The invasive activity of human melanoma cells (cell line A7) upon chitosan treatment was analyzed by a cell-based invasion assay recently described.[9,20] In contrast to the well-known Boyden chamber, this assay uses an electrically tight epithelial monolayer of MDCK cells instead of a reconstituted basement matrix. Permeablization of this tight epithelial cell layer due to the migratory activity of cells was monitored by measuring the transepithelial electrical resistance (TEER). For each experiment, 10^6 melanoma cells with either 20 μg mL^{-1} chitosan (DA 29.4%, MW = 452100 ± 13600 g mol^{-1}, generated and characterized as previously reported[29]) or with the corresponding volume of ultrapure water were seeded close to the basolateral surface of the epithelial monolayer but separated from it by a filter membrane (no physical contact) (Figure 1A).

Within 20 h of coculture with untreated melanoma cells, TEER of the MDCK monolayer decreased rapidly to 11.0 ± 0.3% (n = 6) of its initial value (Figure 1B,1C). However, chitosan-treated cells were less aggressive, reducing TEER to 38 ± 4.3% (n = 6) of its initial value (Figure 1B,1C), reflecting a less pronounced permeabilization of the MDCK monolayer. As melanoma cells were separated from the MDCK monolayer by the filter membrane, the impaired invasiveness cannot be due to decreased cancer cell motility or changes in cancer cell morphology. A simple explanation for the chitosan-related effect would be a pro-apoptotic effect of chitosan on tumor cells. Since it has been shown that chitosan is capable of inducing apoptosis in human bladder tumor cells,[6] a MTT-based proliferation assay was performed to investigate whether chitosan has a comparable effect on human melanoma cells. Therefore, human melanoma cells were incubated with chitosan at a concentration of 20 or 100 μg/mL. However, as shown in Figure 2, proliferation of melanoma cells was not affected by chitosan.

Several studies have shown that cancer cells with high expression levels of MMPs are characterized by enhanced malignancy. We have shown that melanoma cell-derived MMP2 and MMP1 play a pivotal role in tumor progression.[9,11,17]

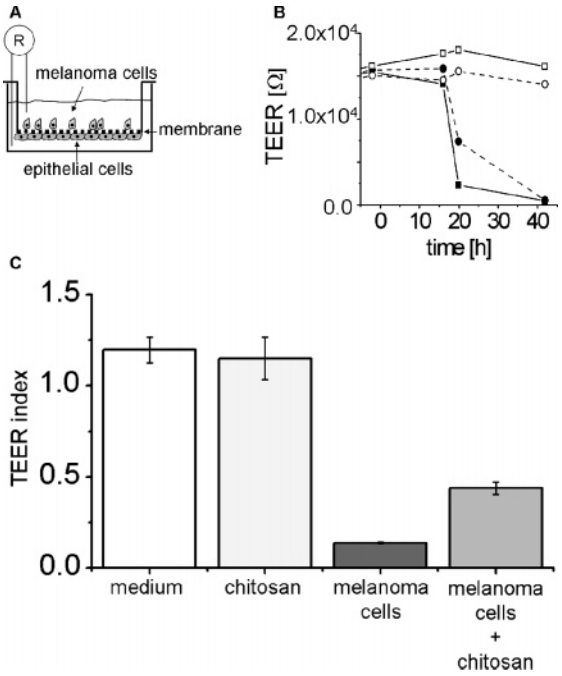

Figure 1. Invasive activity of human melanoma cells toward an epithelial cell layer in the presence or absence of 20 μg mL^{-1} chitosan. (A) Experimental setup for determining the invasive activity by measuring the breakdown of the transepithelial electrical resistance (TEER) in a time dependent manner. (B) Kinetic course of TEER in one representative TEER experiment; melanoma cells (closed symbols) or culure medium without cells (open symbols) and chitosan (circles) or water (squares) were added at time point 0 h. (C) TEER breakdown 20−25 h after melanoma cells were added; TEER index represents TEER breakdown relative to time point 0 h; data given are mean values ± SD of three independent experiments.

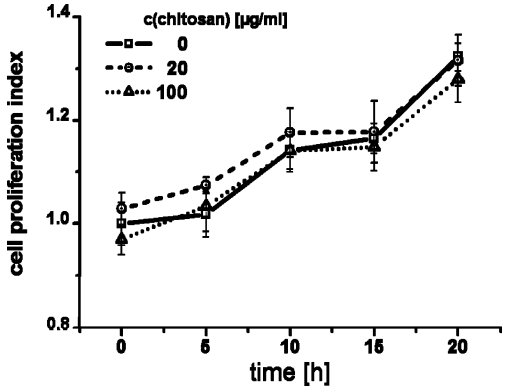

Figure 2. Proliferation of human melanoma cells in the absence (solid line) or presence of 20 (dashed line) or 100 (dotted line) μg/mL chitosan over an incubation period of 20 h. Proliferation was measured by a MTT-based proliferation assay. The diagram represents mean values ± SD of eight independent experiments.

Therefore, a mechanism based on secretion of proteases appears to be crucial for the destruction of the cellular monolayer. In previous studies, we identified MMP2 as being mainly responsible for the destruction of the MDCK monolayer.[9,17]

Chitosan Treatment Decreases MMP2 Content in the Supernatant of Melanoma Cells. The above-described experiments implied that the chitosan-related attenuation of melanoma cell invasion might be due to reduced MMP activity. MMP activity in the supernatant of melanoma cells was, therefore, measured by gelatin zymography. In line with our previous data, we detected a single gelatinolytic band at a molecular weight of 62 kDa, corresponding to active MMP2 (Figure 3A).[17] MMP2 activity was reduced upon incubation with chitosan in a dose

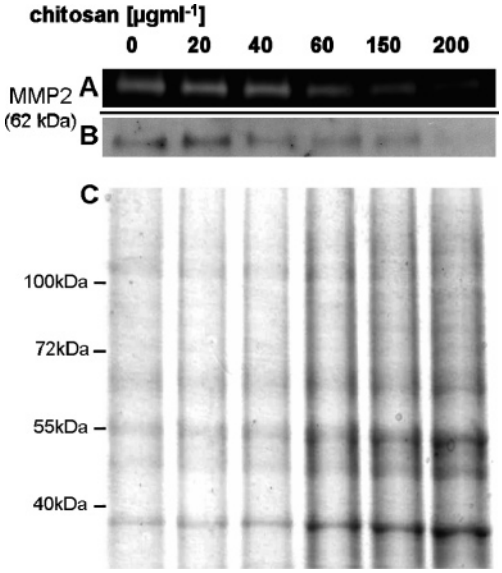

Figure 3. Activity and amount of MMP2 in the supernatant of human melanoma cells in the absence or presence of chitosan (20 to 200 μg mL^{-1}, incubated with the cells for 8 h). (A) Gelatin zymography; (B) immuno blot; (C) Coomassie stained SDS-PAGE gel. In all cases, equal volumes of cell supernatant were applied to the gel.

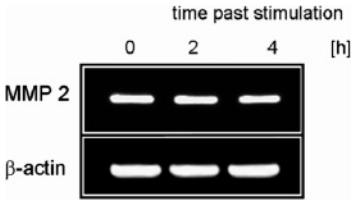

Figure 4. Expression analysis of MMP2 in melanoma cells by means of semiquantitative RT-PCR in the presence of chitosan (20 μg mL^{-1}, incubated for 0, 2, and 4 h).

dependent manner (Figure 3A). Western blot analysis revealed that the reduced MMP2 activity was due to a reduced content of MMP2 protein in the cell supernatant (Figure 3B). However, as shown in Figure 3C, total protein content increases upon chitosan treatment. This indicates that the chitosan-induced decrease of MMP2 amount is not due to a nonspecific reduction of all supernatant proteins. Kim et al. have shown that chitosan oligomers are able to suppress the expression of MMP2 in human fibroblasts.[12] In contrast, other data indicate that chitosan or chitosan oligomers enhance MMP1 activity in human fibroblasts.[30] We performed RT-PCR to investigate whether the decrease in MMP2 activity in the supernatant of chitosan-treated melanoma cells was due to a decrease in MMP2 expression (Figure 4). Expression analysis revealed no decreased MMP2 mRNA level after incubation with chitosan, so that a posttranscriptional effect of chitosan can be assumed. These apparent inconsistencies between different studies may be explained by different chitosans or different cell types used.

MMP2 Chitosan Interaction Imaged by Atomic Force Microscopy. As MMP2 expression in melanoma cells was not affected by chitosan, our data suggest a post-transcriptional effect of chitosan such as a direct physicochemical interaction. Atomic force microscopy (AFM) allows to study the nanostructure of single molecules under native conditions.[31−33] Therefore, we applied AFM to study the interaction between chitosan and MMP2 on a molecular level. In the first set of experiments, pure chitosan or pure MMP2 was immobilized on a freshly cleaved mica surface and analyzed for their molecular dimensions. Representative AFM images of chitosan and MMP2 are

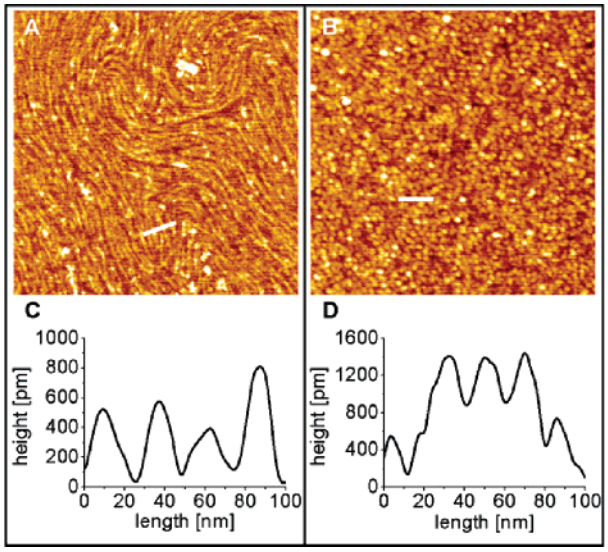

Figure 5. Tapping mode atomic force microscopy of chitosan (A) and MMP2 (B) on freshly cleaved mica surfaces. Resolution was in the range of single molecules as shown by corresponding cross sections of the images (C, D). The white bars (100 nm) mark the position of the cross sections.

shown in Figure 5. In Figure 5A, a tightly packed filamentous network of putative single chitosan molecules is visible. The diameter and height of single filaments was 26.6 ± 7.58 nm (n = 10) and 0.6 ± 0.09 nm (n = 10), respectively. These data agree with previously reported AFM measurements of single polymer chains of hyaluronan (diameter >10 nm; height 0.6 ± 0.1 nm).[34,35] In comparison, the diameter and height of single MMP2 molecules was 16.0 ± 1.55 nm (n = 20) and 1.1 ± 0.31 nm (n = 20), respectively (Figure 5B). These molecular dimensions of individual MMP2 molecules correspond to a molecular volume of 113.0 ± 60.9 nm^3. This experimentally determined molecular volume is almost identical to the theoretical volume of 117.4 nm^3 as calculated based on the molecular weight of active MMP2 (62 kDa).[26] A possible change in morphology or size of the individual molecules during an interaction between chitosan and MMP2 was studied by AFM analysis of a mixture of the two polymers. AFM images of the MMP2−chitosan solution revealed large globular structures as shown in Figure 6A, possibly formed by a complexation of MMP2 by chitosan. The diameter and height of these complexes was 349.0 ± 69.06 nm and 26.5 ± 11.50 nm (n = 15), respectively (Figure 6C). Apart from these large structures, we detected very small aggregates with a height of less than 10 nm probably representing an intermediate state of the final complex. Tapping mode AFM allowed the generation of phase images to characterize the chitosan−MMP2 particles in a biophysical manner. The phase images shown in Figure 6D represent the interference between the scanning tip and the imaged surface. Interestingly, single complexes revealed a sharply defined but irregularly shaped core (see black arrow in Figure 6D) surrounded by a homogeneous circular shell (see white arrow in Figure 6D). These data indicate that the chitosan−MMP2 aggregates consist of a crystalline-like core embedded in an amorphous capsule. We speculate that the phase shift (bright regions) at the shell of the particles is related to a strong electrostatic interaction between unbound chitosan chains and the scanning tip. The missing phase shift at the core of the particles (black regions) might indicate diminished electrostatic properties due to the binding of MMP2 to chitosan. However,

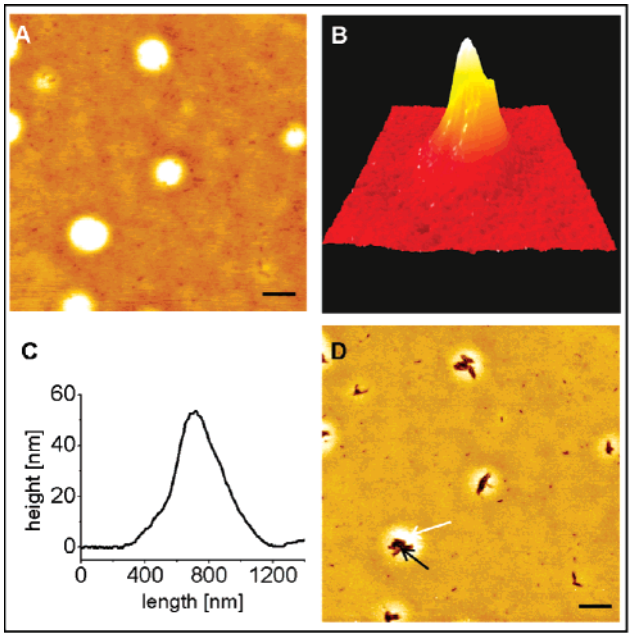

Figure 6. Tapping mode atomic force microscopy of a MMP2 chitosan complex. (A) Height image; white square indicates the position of the three-dimensional view (B); white arrows indicate the position of the cross section (C); (D) phase image obtained for the same area as given in part A; black arrow points to the core, white arrow to the shell of the core/shell type complex. The black bar in parts A and D corresponds to 500 nm.

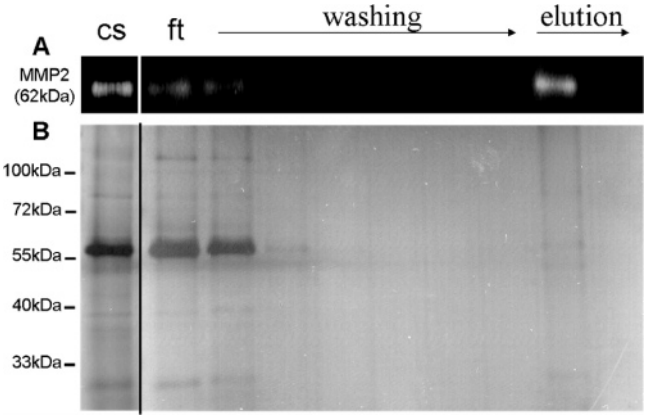

Figure 7. Affinity chromatography of melanoma cell supernatant in a column packed with chitosan beads. cs: Cell supernatant; ft: flow through fraction; the column was washed with eight 1-mL fractions of HEPES buffer prior to elution of bound proteins using two 1-mL fractions of HEPES buffer containing 1% SDS. (A) Gelatin zymography; (B) silver-stained SDS-PAGE gel.

an exact interpretation of phase image data is still under discussion[36] and further studies are needed to confirm our hypothesis.

Specific MMP2-Chitosan Interaction Shown by Affinity Chromatography. AFM images indicated a binding of MMP2 to chitosans. To support these data, we analyzed the binding specificity and affinity of chitosan to MMP2 by liquid affinity chromatography. The affinity column composed of macroscopic chitosan beads was loaded with melanoma cell-derived supernatant. Since cell supernatant was generated in a physiological buffer solution, column-bound proteins were eluted stepwise using the same buffer. Finally, proteins with high affinity to the chitosan, were elute using the same buffer containing 1% SDS (last two elution steps in Figure 7). The collected fractions were analyzed for their protein content (SDS-PAGE) and MMP2 activity (gelatin zymography) (Figure 7A,B). Prior to affinity chromatography, the cell supernatant (cs) was rich in protein and showed a strong gelatinolytic band due to high MMP2 activity (Figure 7A). In the flow-through fraction (ft) and in the first elution fraction of the chromatography, only weak MMP2 activity was detectable (Figure 7A) in contrast to high protein contents (Figure 7B). The characteristic protein pattern of the cell supernatant is also visible in these fractions (Figure 7B), indicating that the bulk of supernatant proteins did not bind to the chitosan column. In contrast, low MMP2 activity levels in the flow through and the first elution fraction indicate a high affinity of MMP2 to the chitosan. In the following elution steps, no further protein or MMP2 activity was detected. As mentioned above, we then used SDS in the mobile phase to recover all column bound proteins. Already the first elution with SDS revealed a high MMP2 activity band in the zymography assay (Figure 7A). In contrast, virtually no clear protein band could be detected (Figure 7B). These affinity chromatography experiments showed that chitosan retains melanoma cell-derived MMP2 in a specific manner and with relatively high affinity since complete recovery required the presence of SDS in the elution buffer. The binding of chitosan to MMP2 could be explained by the interaction between the chitosan and the Zn^{2+}–ion that is coordinated within the catalytic domain of MMPs.[37] Chelation of divalent ions such as copper or zinc by chitosan is a known and well-studied phenomenon[38,39] that has already been applied for wastewater treatment to clear the water from heavy metal ions.[40] Recently, a detailed study analyzing the binding mechanism of copper and chitosan monomer[41] showed that the binding between copper and the uncharged amino group of the glucosamine residue is favored. However, we cannot exclude other binding mechanisms between chitosan and MMP2.

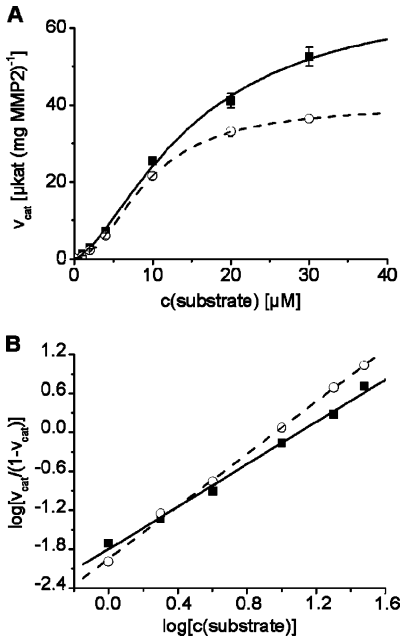

Figure 8. Enzyme kinetic of recombinant MMP2 in the presence of different concentrations of a synthetic thiopeptolide substrate. (A) Enzyme activity; (B) Hill plot. Data given represent mean values ± SD of three independent experiments.

Peptidolytic Activity of MMP2 is Reduced in the Presence of Chitosan. A colorimetric MMP2 activity assay was performed to analyze whether the observed physicochemical interaction between chitosan and MMP2 also influences the hydrolytic activity of MMP2. As shown in Figure 8A the turnover rate of the substrate increased with increasing substrate concentration. However, substrate dose dependency of the hydrolytic activity of MMP2 proceeded in a sigmoidal manner

indicating a cooperative substrate binding, a characteristic for non Michaelis−Menten behavior. V_{max} in the absence of chitosan was 62.8 ± 7.65 μkat (mg MMP2)$^{-1}$. In contrast, V_{max} was reduced in the presence of chitosan to 39.8 ± 0.55 μkat (mg MMP2)$^{-1}$ corresponding to a reduction of about 42%. K_{50} was elevated in the presence of chitosan from 15.1 ± 2.59 to 24.1 ± 2.19 μM. These data indicate that the interaction between chitosan and MMP2 also influences the hydrolytic activity of the protease. The observed cooperativity might be related to cooperative binding of the substrate to the three tandem fibronectin Type II repeats present in MMP2.[42] Such cooperativity can be described by the Hill coefficient n_H obtained by Hill plot analysis as shown in Figure 8B. In chitosan-free reaction buffer, n_H was 1.6 ± 0.05, while it was 2.0 ± 0.08 in the presence of chitosan, indicating an increase in cooperativity of substrate binding upon chitosan treatment. We speculate that the shift of n_H might be related to a disturbance of the spatial orientation of the substrate binding domains of MMP2 due to chitosan binding.

Conclusion

The present study shows that treatment of highly invasive human melanoma cells with chitosan attenuates their invasive properties. As previously reported, the invasive activity of tumor cells can be reduced by inhibition of MMPs using artificial MMP inhibitors (MMPIs) such as ilomastat.[9] Therefore, inhibition of MMPs is currently a major goal in cancer drug research. However, to date, the application of MMPIs in clinical trials revealed strong adverse effects precluding further testing.[43,44] A challenge for future MMPI development, thus, lies in the identification of new inhibitors with alternative inhibition mechanisms. The enzyme kinetic measurements presented here show that chitosan reduces the hydrolytic activity of MMP2 because of a direct molecular interaction. Future research might validate chitosan as an alternative MMPI by elucidating the chitosan MMP2 binding mechanism. Beside their role in tumor cell invasion, MMPs are also involved in wound healing[45] where pathological MMP regulation results in chronic ulcerations.[46] Since chitosan is known to improve wound healing, we speculate that the MMP binding capacity of chitosan is at least partly responsible for the improved wound healing mediated by chitosan-based wound dressings.

Acknowledgment. We thank JPK Instruments, Berlin, Germany, for generous support of the AFM laboratory in the Department of Dermatology, University of Münster, and Dr. G. Lamarque, University of Claude Bernard Lyon 1, France, for generously providing the chitosan. This work is part of the European Research Project NanoBioSaccharides financially supported by the 6th Framework Research Programme of the European Union.

References and Notes

(1) McKay, G.; Ho, Y. S.; Ng, J. C. Y. *Sep. Purif. Methods* **1999**, *1*, 87−125.
(2) Dutta, P. K.; Ravikumar, M. N.; Dutta, J. *J. Macromol. Sci.-Polym. Rev.* **2002**, *3*, 307−354.
(3) Muzzarelli, R. A.; Mattioli-Belmonte, M.; Pugnaloni, A.; Biagini, G. *EXS* **1999**, 251−264.
(4) Amaral, I. F.; Sampaio, P.; Barbosa, M. A. *J. Biomed. Mater. Res. A.* **2006**, *2*, 335−346.
(5) Howling, G. I.; Dettmar, P. W.; Goddard, P. A.; Hampson, F. C.; Dornish, M.; Wood, E. J. *Biomaterials* **2001**, *22*, **2959−2966**.
(6) Takimoto, H.; Hasegawa, M.; Yagi, K.; Nakamura, T.; Sakaeda, T.; Hirai, M. *Drug Metab. Pharmacokinet.* **2004**, *1*, 76−82.
(7) Dhiman, H. K.; Ray, A. R.; Panda, A. K. *Biomaterials* **2004**, *21*, 5147−5154.
(8) Dhiman, H. K.; Ray, A. R.; Panda, A. K. *Biomaterials* **2005**, *9*, 979−986.
(9) Ludwig, T.; Ossig, R.; Graessel, S.; Wilhelmi, M.; Oberleithner, H.; Schneider, S. W. *Am. J. Physiol. Renal Physiol.* **2002**, *2*, F319−27.
(10) Hofmann, U. B.; Houben, R.; Brocker, E. B.; Becker, J. C. *Biochimie* **2005**, *3−4*, 307−314.
(11) Goerge, T.; Barg, A.; Schnaeker, E. M.; Poppelmann, B.; Shpacovitch, V.; Rattenholl, A.; Maaser, C.; Luger, T. A.; Steinhoff, M.; Schneider, S. W. *Cancer Res.* **2006**, *15*, 7766−7774.
(12) Kim, M. M.; Kim, S. K. *FEBS Lett.* **2006**, *11*, 2661−2666.
(13) Sternlicht, M. D.; Werb, Z. *Annu. Rev. Cell Dev. Biol.* **2001**, 463−516.
(14) Page-McCaw, A.; Ewald, A. J.; Werb, Z. *Nat. Rev. Mol. Cell Biol.* **2007**, *3*, 221−233.
(15) Hofmann, U. B.; Westphal, J. R.; Van Muijen, G. N.; Ruiter, D. J. *J. Invest. Dermatol.* **2000**, *3*, 337−344.
(16) Deryugina, E. I.; Quigley, J. P. *Cancer Metastasis Rev.* **2006**, *1*, 9−34.
(17) Schnaeker, E. M.; Ossig, R.; Ludwig, T.; Dreier, R.; Oberleithner, H.; Wilhelmi, M.; Schneider, S. W. *Cancer Res.* **2004**, *24*, 8924−8931.
(18) Cunningham, C. C.; Gorlin, J. B.; Kwiatkowski, D. J.; Hartwig, J. H.; Janmey, P. A.; Byers, H. R.; Stossel, T. P. *Science* **1992**, *5042*, 325−327.
(19) Gekle, M.; Wunsch, S.; Oberleithner, H.; Silbernagl, S. *Pflugers Arch.* **1994**, *2*, 157−162.
(20) Zak, J.; Schneider, S. W.; Eue, I.; Ludwig, T.; Oberleithner, H. *Pflugers Arch.* **2000**, *1*, 179−183.
(21) Mosmann, T. *J. Immunol. Methods* **1983**, *1−2*, 55−63.
(22) Chomczynski, P.; Sacchi, N. *Anal. Biochem.* **1987**, *1*, 156−159.
(23) Mullis, K. B.; Faloona, F. A. *Methods Enzymol.* **1987**, 335−350.
(24) Heukeshoven, J.; Dernick, R. *Electrophoresis* **1988**, *1*, 28−32.
(25) Blakesley, R. W.; Boezi, J. A. *Anal. Biochem.* **1977**, *2*, 580−582.
(26) Schneider, S. W.; Larmer, J.; Henderson, R. M.; Oberleithner, H. *Pflugers Arch.* **1998**, *3*, 362−367.
(27) Schneider, S.; Folprecht, G.; Krohne, G.; Oberleithner, H. *Pflugers Arch.* **1995**, *5*, 795−801.
(28) Weingarten, H.; Feder, J. *Anal. Biochem.* **1985**, *2*, 437−440.
(29) Lamarque, G.; Lucas, J. M.; Viton, C.; Domard, A. *Biomacromolecules* **2005**, *1*, 131−142.
(30) Okamura, Y.; Nomura, A.; Minami, S.; Okamoto, Y. *Biomacromolecules* **2005**, *5*, 2382−2384.
(31) Muller, D. J.; Heymann, J. B.; Oesterhelt, F.; Moller, C.; Gaub, H.; Buldt, G.; Engel, A. *Biochim. Biophys. Acta* **2000**, *1*, 27−38.
(32) Schillers, H.; Danker, T.; Madeja, M.; Oberleithner, H. *J. Membr. Biol.* **2001**, *3*, 205−212.
(33) Muller, D. J.; Sapra, K. T.; Scheuring, S.; Kedrov, A.; Frederix, P. L.; Fotiadis, D.; Engel, A. *Curr. Opin. Struct. Biol.* **2006**, *4*, 489−495.
(34) Gunning, A. P.; Morris, V. J.; AlAssaf, S.; Phillips, G. O. *Carbohydr. Polym.* **1996**, *1*, 1−8.
(35) Cowman, M. K.; Li, M.; Balazs, E. A. *Biophys. J.* **1998**, *4*, 2030−2037.
(36) Wang, Y.; Song, R.; Li, Y. S.; Shen, J. S. *Surf. Sci.* **2003**, *3*, 136−148.
(37) Nagase, H.; Visse, R.; Murphy, G. *Cardiovasc. Res.* **2006**, *3*, 562−573.
(38) Findon, A.; Mckay, G.; Blair, H. S. *J. Environ. Sci. Health Part A: Environ. Sci. Eng. Toxic Hazard. Subst. Control* **1993**, *1*, 173−185.
(39) Inoue, K.; Baba, Y.; Yoshizuka, K. *Bull. Chem. Soc. Jpn.* **1993**, *10*, 2915−2921.
(40) Muzzarel.Ra; Sipos, L. *Talanta* **1971**, *9*, 853.
(41) Terreux, R.; Domard, M.; Viton, C.; Domard, A. *Biomacromolecules* **2006**, *1*, 31−37.
(42) Gehrmann, M. L.; Douglas, J. T.; Banyai, L.; Tordai, H.; Patthy, L.; Llinas, M. *J. Biol. Chem.* **2004**, *45*, 46921−46929.
(43) Fisher, J. F.; Mobashery, S. *Cancer Metastasis Rev.* **2006**, *1*, 115−136.
(44) Overall, C. M.; Kleifeld, O. *Br. J. Cancer* **2006**, *7*, 941−946.
(45) Kahari, V. M.; Saarialho-Kere, U. *Exp. Dermatol.* **1997**, *5*, 199−213.
(46) Trengove, N. J.; Stacey, M. C.; MacAuley, S.; Bennett, N.; Gibson, J.; Burslem, F.; Murphy, G.; Schultz, G. *Wound Repair Regen.* **1999**, *6*, 442−452.

BM0703214